Navier-Stokes Solutions for Laminar Incompressible Flows in Forward-Facing Step Geometries

R. W. Mei*
University of Illinois, Urbana, Illinois
and
A. Plotkin†
San Diego State University, San Diego, California

Two-dimensional laminar flow of an incompressible fluid through channels with symmetrical and asymmetrical sudden constrictions formed by a semi-infinite step change in width, and flow through a cascade formed by an infinite stack of finite-thickness flat plates, is investigated using a finite-difference method. The Navier-Stokes equations in conservation form and body-fitted coordinates are solved up to a critical Reynolds number beyond which the flow may become unsteady. The numerical scheme is related to a second-order-accurate, artificial diffusion-free scheme previously developed by the present authors. Results are obtained that resolve the separated flowfield upstream and downstream of the step.

Introduction

THERE is still much interest in the accurate computation of two-dimensional laminar incompressible flows in internal configurations dominated by streamwise convection possibly containing regions of separated flow. A standard model problem is the symmetrical sudden channel expansion formed by a semi-infinite step increase in width. Accurate solutions to the Navier-Stokes equations for moderate to large Reynolds numbers are given by Ghia et al. in Ref. 1 wherein reference to previous work is given. Channels with forward-facing step geometries (channel constriction) have received much less attention in the literature even though their solutions may possess flow separation both upstream and downstream of the step.

In this paper we consider two-dimensional laminar incompressible flows through channels with symmetrical (case I) and asymmetrical (case II) sudden constrictions (formed by a semi-infinite step), and flow through a cascade (case III) formed by a stack of semi-infinite flat plates of finite thickness. The Navier-Stokes equations in stream function-vorticity form in orthogonal curvilinear coordinates are solved using a finite-difference method for moderate to high Reynolds number, Re, values.

The symmetrical sudden constriction case has been investigated carefully by Dennis and Smith,[2] where results from both finite-difference and large-Reynolds-number asymptotic methods are presented and compared. The agreement between numerical and analytical results is fairly good for the upstream part (before the step), however, the numerical results are not satisfactory for the downstream part, even though a very fine grid is used (80 intervals across the upstream channel).

The numerical method used in the present studies is essentially the one developed by Mei and Plotkin[3] with a slight modification to the streamwise convection term. Instead of using central differences for convection in the streamwise direction, we use second-order upwind differences. The resulting finite-difference equation is artificial diffusion-free. The application to the present streamwise convection-dominant problem is successful.

Received June 5, 1985; revision received Oct. 14, 1985; presented as Paper 86-0110 at the AIAA 24th Aerospace Sciences Meeting, Reno, NV, Jan. 6-9, 1986.

*Graduate Student, Department of Mechanical and Industrial Engineering.

†Professor and Chairman, Department of Aerospace Engineering and Engineering Mechanics. Associate Fellow AIAA.

Governing Equations in Orthogonal Coordinates

In this study, the two-dimensional, steady, laminar incompressible Navier-Stokes equations are solved numerically in terms of vorticity ω and stream function ψ. The vorticity transport equation in conservation form is

$$\frac{\partial \omega}{\partial t} + \nabla \cdot (V\omega) = \frac{1}{Re}\nabla^2 \omega \tag{1}$$

The governing equation for ψ,

$$\nabla^2 \psi = -\omega \tag{2}$$

is modified to

$$\frac{\partial \psi}{\partial t} = \mu(\nabla^2 \psi + \omega) \tag{3}$$

to seek the final steady solution, where μ is a fictitious positive diffusion coefficient which can be chosen arbitrarily for convenience. The velocity V is related to the stream function by

$$V = \nabla \psi \times k \tag{4}$$

where k is the unit vector normal to the plane of flow.

There are several advantages to the use of body-fitted coordinates, and the governing equations [Eqs. (1), (3), and (4)] in general orthogonal coordinates (ξ_1, ξ_2) are

$$h_1 h_2 \frac{\partial \omega}{\partial t} + \frac{\partial}{\partial \xi_1}(u\omega) + \frac{\partial}{\partial \xi_2}(v\omega) = \frac{1}{Re}\left[\frac{\partial}{\partial \xi_1}\left(\frac{h_2}{h_1}\frac{\partial \omega}{\partial \xi_1}\right) + \frac{\partial}{\partial \xi_2}\left(\frac{h_1}{h_2}\frac{\partial \omega}{\partial \xi_2}\right)\right] \tag{5}$$

$$h_1 h_2 \frac{\partial \psi}{\partial t} = \mu\left[\frac{\partial}{\partial \xi_1}\left(\frac{h_2}{h_1}\frac{\partial \psi}{\partial \xi_1}\right) + \frac{\partial}{\partial \xi_2}\left(\frac{h_1}{h_2}\frac{\partial \psi}{\partial \xi_2}\right) + h_1 h_2 \omega\right] \tag{6}$$

$$u=\frac{\partial\psi}{\partial\xi_2} \qquad v=-\frac{\partial\psi}{\partial\xi_1} \tag{7}$$

where u,v are not the physical velocity components, and h_1 and h_2 are defined as

$$h_i^2=\left(\frac{\partial x}{\partial\xi_i}\right)^2+\left(\frac{\partial y}{\partial\xi_i}\right)^2 \qquad i=1,2 \tag{8}$$

and (x,y) are the Cartesian coordinates.

Numerical Algorithm

The finite-difference method developed by Mei and Plotkin[3] is essentially applied here to seek the steady-state solution of Eqs. (5-7). The discretized form of the equations in the general coordinates is given below to indicate the method.

$$\begin{aligned}
&h_{1i,j}h_{2i,j}\frac{\omega_{i,j}^{n+1}-\omega_{i,j}^{n}}{\Delta t}+\frac{\partial(u\omega)}{\partial\xi_{1i,j}}\\
&+\frac{v_{i,j+1}^{n}\omega_{i,j+1}^{n}-v_{i,j}^{n}\omega_{i,j}^{n}+v_{i,j}^{n}\omega_{i,j}^{n+1}-v_{i,j-1}^{n}\omega_{i,j-1}^{n+1}}{2\Delta\xi_2}\\
&=\frac{1}{Re\Delta\xi_1^2}\left\{\left(\frac{h_2}{h_1}\right)_{i+\frac12,j}\omega_{i+1,j}^{n}-\left[\left(\frac{h_2}{h_1}\right)_{i+\frac12,j}\right.\right.\\
&\left.+\left(\frac{h_2}{h_1}\right)_{i-\frac12,j}\right]\omega_{i,j}^{n+1}+\left(\frac{h_2}{h_1}\right)_{i-\frac12,j}\omega_{i-1,j}^{n+1}\Bigg\}\\
&+\frac{1}{Re\Delta\xi_2^2}\left\{\left(\frac{h_1}{h_2}\right)_{i,j+\frac12}\omega_{i,j+1}^{n}-\left[\left(\frac{h_1}{h_2}\right)_{i,j+\frac12}\right.\right.\\
&\left.\left.+\left(\frac{h_1}{h_2}\right)_{i,j-\frac12}\right]\omega_{i,j}^{n+1}+\left(\frac{h_1}{h_2}\right)_{i,j-\frac12}\omega_{i,j-1}^{n+1}\right\}
\end{aligned} \tag{9}$$

$$\begin{aligned}
&h_{1i,j}h_{2i,j}\frac{\psi_{i,j}^{n+1}-\psi_{i,j}^{n}}{\Delta t}=\frac{\mu}{\Delta\xi_1^2}\left\{\left(\frac{h_2}{h_1}\right)_{i+\frac12,j}\psi_{i+1,j}^{n}\right.\\
&-\left[\left(\frac{h_1}{h_2}\right)_{i+\frac12,j}+\left(\frac{h_2}{h_1}\right)_{i-\frac12,j}\right]\psi_{i,j}^{n+1}\Bigg\}\\
&\left.+\left(\frac{h_2}{h_1}\right)_{i-\frac12,j}\psi_{i-1,j}^{n+1}\right\}+\frac{\mu}{\Delta\xi_2^2}\left\{\left(\frac{h_1}{h_2}\right)_{i,j+\frac12}\psi_{i,j+1}^{n}\right.\\
&-\left[\left(\frac{h_1}{h_2}\right)_{i,j+\frac12}+\left(\frac{h_1}{h_2}\right)_{i,j-\frac12}\right]\psi_{i,j}^{n+1}\\
&\left.+\left(\frac{h_1}{h_2}\right)_{i,j-\frac12}\psi_{i,j-1}^{n+1}\right\}+\mu h_{1i,j}h_{2i,j}\omega_{i,j}^{n+1}
\end{aligned} \tag{10}$$

$$u_{i,j}^{n+1}=(\psi_{i,j+1}^{n+1}-\psi_{i,j-1}^{n+1})/(2\Delta\xi_2)$$

$$v_{i,j}^{n+1}=-(\psi_{i+1,j}^{n+1}-\psi_{i-1,j}^{n+1})/(2\Delta\xi_1) \tag{11}$$

In Ref. 3, the streamwise convection term is represented as

$$\frac{u_{i+1,j}^{n}\omega_{i+1,j}^{n}-u_{i,j}^{n}\omega_{i,j}^{n}+u_{i,j}^{n}\omega_{i,j}^{n+1}-u_{i-1,j}^{n}\omega_{i-1,j}^{n+1}}{2\Delta\xi_1} \tag{12}$$

However, in the present streamwise convection-dominated problem this central difference representation leads to a solution with wiggles at certain Reynolds numbers. In addition, note that the normal component of velocity is usually small relative to the streamwise component in the transformed coordinates. Thus, Eq. (12) is changed to the following form while $\partial v\omega/\partial\xi_2$ is still represented by central differences.

$$\begin{aligned}
\left.\frac{\partial(u\omega)}{\partial\xi_1}\right|_{i,j}&=\frac{3u_{i,j}^{n}\omega_{i,j}^{n+1}-4u_{i-1,j}^{n}\omega_{i-1,j}^{n+1}+u_{i-2,j}^{n}\omega_{i-2,j}^{n+1}}{2\Delta\xi_1} \quad \text{if } u_{i,j}^{n}\geq 0\\
&=-\frac{3u_{i,j}^{n}\omega_{i,j}^{n+1}-4u_{i+1,j}^{n}\omega_{i+1,j}^{n+1}+u_{i+2,j}^{n}\omega_{i+2,j}^{n+1}}{2\Delta\xi_1} \quad \text{if } u_{i,j}^{n}<0
\end{aligned} \tag{13}$$

The use of Eq. (13) eliminated the appearance of wiggles afterward.

For convection-dominated or high-Peclet-number problems, there are various methods to treat the convection term, e.g., first-order upwind, central difference, QUICK, skewed upwind, and second-order upwind. In Ref. 4, Shyy gave a detailed discussion of the preceding methods applied to model problems and concluded that the second-order upwind method was the best among the five methods. It is the authors' belief that from the present study, the second-order upwind method works quite well for streamwise convection-dominated problems, especially in the presence of geometry singularities that affect the downstream flowfield.

Model Problems

Coordinate Transformation

Three different types of confined laminar flows are investigated herein. They are the flow through a channel with a symmetrical sudden constriction (case I) which was considered by Dennis and Smith,[2] with an asymmetrical sudden constriction (case II), and flow over a cascade (case III) as shown in Figs. 1a, 1b, and 1c, respectively. The geometries are almost the same and the difference between the cases lies in the specification of the boundary conditions.

The body-fitted coordinates are set up by conformal mapping as follows:

$$\zeta=\eta_1+i\eta_2, \qquad \tau=\left[\frac{\zeta+b^2}{\zeta+1}\right]^{\frac12}$$

$$z=x+iy=\frac{1}{\pi}\left[\frac{1}{b}\ln\frac{b+\tau}{b-\tau}-\ln\frac{1+\tau}{1-\tau}\right] \tag{14}$$

where $b=1/H$. Equation (14) maps the doubly infinite forward-step channel in (x,y) coordinates onto a doubly infinite strip in (η_1,η_2) coordinates.

In order to apply the upstream and downstream boundary conditions far enough away from the step, and to resolve the flow around corners, another transformation in the stream-

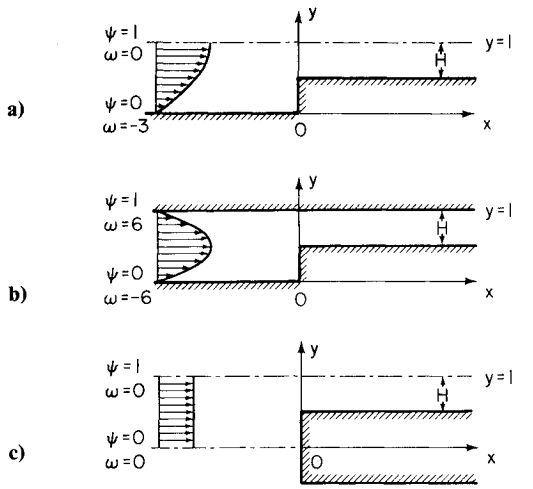

Fig. 1 Geometry and coordinate system: a) symmetrical constriction; b) asymmetrical constriction; c) cascade.

wise direction is made

$$\xi_1 = \frac{1}{2\pi}\left[\tan^{-1}\frac{\eta_1-\alpha_1}{D_1}+\tan^{-1}\frac{\eta_1-\alpha_2}{D_2}\right]+\frac{1}{2} \tag{15}$$

which maps $-\infty<\eta_1<\infty$ onto $0<\xi_1<1$.

Normal stretching can be made as follows to resolve the wall layer

$$\xi_2 = 1-\left(\tan\frac{1-\eta_2}{c}\Big/\tan\frac{1}{c}\right) \tag{16a}$$

for cases I and III, while

$$\xi_2 = \frac{1}{2}+\left(\tan\frac{\eta-\frac{1}{2}}{c}\Big/2\tan\frac{1}{2c}\right) \tag{16b}$$

is used for the asymmetrical sudden constriction (case II), which stretches both the upper ($\eta_2=1$) and lower ($\eta_2=0$) walls. The rules to select the parameters in Eqs. (15 and 16) are similar to those in Ref. 1 and thus are not described here.

Boundary Conditions

Fully developed laminar flow (Poiseuille profiles) is assumed far upstream and downstream for the channel geometries and far downstream for the cascade. A uniform stream is assumed far upstream for the cascade.

Vorticity on the solid wall is evaluated by

$$\omega_b = \frac{1}{(h_1h_2)_b}\frac{\partial}{\partial\xi_2}\left(\frac{h_1}{h_2}\frac{\partial\psi}{\partial\xi_2}\right)_b = -2(\psi_{b+1}-\psi_b)/(h_2\Delta\xi_2)^2 \tag{17}$$

which gives satisfactory results although it is first-order accurate. The streamwise velocity component one grid away from the solid wall is calculated from

$$u_{b+1} = (4\psi_{b+1}+\psi_{b+2}-5\psi_b)/(4\Delta\xi_2) \tag{18}$$

as given in Ref. 5.

A converged solution is assumed when

$$\max_{i,j}\frac{|\omega_{i,j}^{n+1}-\omega_{i,j}^{n}|}{\max(1,|\omega_{i,j}^{n}|)} \le 10^{-4}$$

Usually, when the flow separates downstream, it is the grid near the reattachment point on the wall that requires the most iterations.

Results and Discussion

Symmetric Sudden Constriction

For case I, numerical and analytical results have been obtained by Dennis and Smith[2] using the numerical scheme of Dennis and Hudson.[6] The results agree quite well between the numerical and analytical predictions for flow properties upstream of the step, such as the upstream eddy size and wall vorticity. However, the results were less satisfactory downstream of the step at higher Reynolds numbers. For example, the downstream separation, which is a feature of the asymptotic theory, was not obtained at $Re=500$ even with the fine grid size of $h=1/80$. Dennis and Smith[2] claimed that further calculations would be needed in that region of the flow.

In this study of the symmetric constriction, 20 intervals across the channel are used (while 30 intervals were used at $Re=100$ to confirm the fact that 20 are enough). Use of the stretching transformation of Eq. (16a) with $c=0.8$ yields very fine grids near the wall where large gradients exist.

A typical streamline contour is shown in Fig. 2 for $Re=480$ and $H=0.5$. A relatively thin eddy downstream of the step (not obtained numerically at $Re=500$ in Ref. 2) is clearly seen in the printout for stream function through five to six grid points in the normal direction. For the upstream part of the flow, the present results agree very well with the numerical results of Dennis and Smith[2] for the wall vorticity and the size of the eddy, L, defined in Fig. 2. The comparison of L between the present results and those in Ref. 2 is shown in Fig. 3. In Fig. 4, the wall vorticity after the step is shown for various values of Re up to 480 and $H=0.5$. Downstream separation seems to occur at a Reynolds number slightly larger than 230. As Re increases, the reattachment points go further downstream while the separation points approach the convex corner. For $Re\ge400$, it can be observed that there exists an extremely large vorticity gradient slightly after the corner and $\partial\omega_b/\partial x$ is discontinuous. Due to the "singular" behavior of the vorticity near the corner, when $Re\ge485$ no steady solutions are obtainable and instead a periodic vortex shedding from the corner starts to occur. This phenomenon is not unreasonable because near the wall the velocity is vanishingly small, and because the vorticity is exceedingly large near the corner the time-derivative term in the vorticity transport equation [Eq. (1)] is needed to balance the equation. Periodic changes in the vorticity in successive iterations were observed near the corner, but were confined to a local region of three or four grid points. Due to the cluster of grids near the convex corner in both the streamwise and normal directions, this region constitutes only a small part of the computational domain. For example, at $Re=500$ the region of unsteadiness is about $\mathcal{O}(0.014\times0.007)$ in a computational space of $\mathcal{O}(20\times1)$. Thus, general features of the global flowfield, such as the downstream reattachment point, can still be obtained from the computed results.

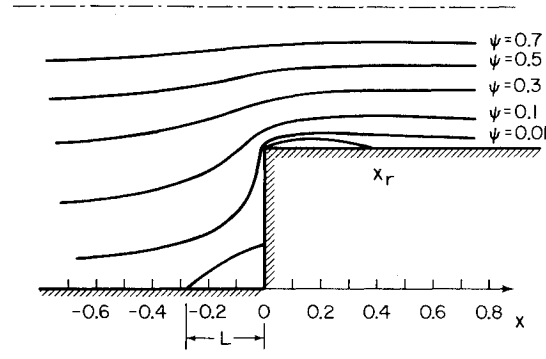

Fig. 2 Streamlines for flow in channel with symmetrical constriction ($Re=480$, $H=0.5$).

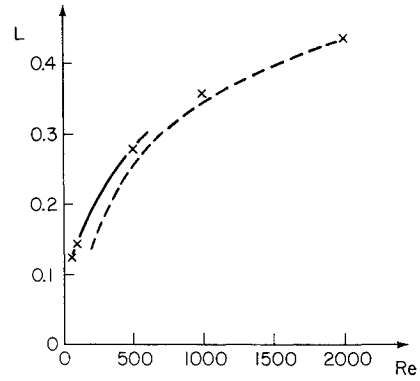

Fig. 3 Comparison of upstream eddy length for symmetrical constriction ($H=0.5$); x numerical, Ref. 2; --- asymptotic, Ref. 2; —— present.

Let x_r be the downstream reattachment point on the wall. The variation of x_r with Reynolds number can be seen in Fig. 5. The lower branch indicates the separation points. The linearity between x_r and Re [which is also a feature of the asymptotic theory (see Smith[7] for the flow in a symmetrical tube constriction)] can be seen clearly for $Re > 300$.

Although the flow becomes unsteady, which cannot be handled by the present scheme, it is observed from the computational results that the movement of the downstream reattachment point is so small that x_r varies only in the third decimal place and, thus, the graphical accuracy of x_r vs Re in Fig. 5 for the unsteady part can be expected to be as good as the steady part.

In order to investigate the effect of grid size, 30 intervals across the channel are also used for $Re = 100$. The wall vorticity comparison between 20 and 30 intervals is exceptionally good. The wall vorticity at different locations (both upstream and downstream of the step) is presented in Table 1. One can clearly see the close agreement even around the corner where the vorticity is singular. From this, we may expect that 20 intervals across the channel are adequate to obtain reasonable resolution even for the downstream flowfield.

When Dennis and Hudson's scheme was used, as the mesh was refined (40-60 intervals, 60-80), the change in the wall vorticity near the corner was not small, as can be seen even at $Re = 100$ in Fig. 5 of Ref. 2. At $Re = 500$, the difference is more dramatic and no separation was observed even with 80 intervals. This could be due to the interaction of false diffusion (that scheme has a large false diffusion at higher Re if the grid size is not small enough) and the corner singularity. As Castro[8] points out, one of the difficulties in numerical predictions of flows with complex geometries (such as the present one with sharp convex corners) is that any error due to the singularities not only affects the local solution but also will be propagated by convection and diffusion to affect the downstream flowfield.

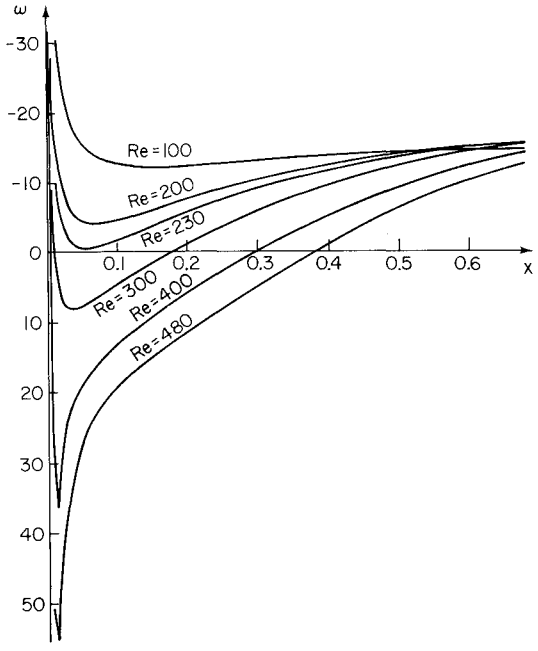

Fig. 4 Wall vorticity after step in symmetrical constriction ($H = 0.5$).

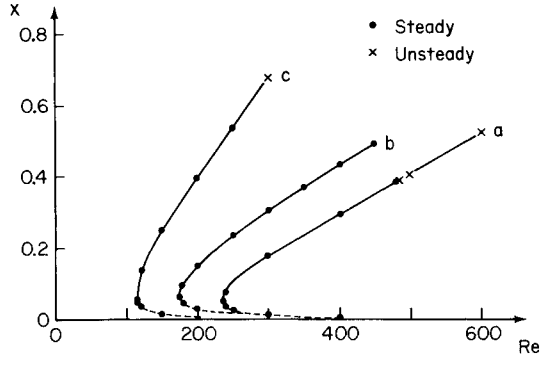

Fig. 5 Dependence of downstream eddy size on Re; —— reattachment points; --- separation points: a, symmetrical constriction; b, asymmetrical constriction; c, cascade ($H = 0.5$).

Asymmetrical Sudden Constriction

The character of the flow in a channel with an asymmetrical constriction is much different from that of the symmetrical constriction whose symmetry line ($\omega = 0$) is replaced by a solid wall.

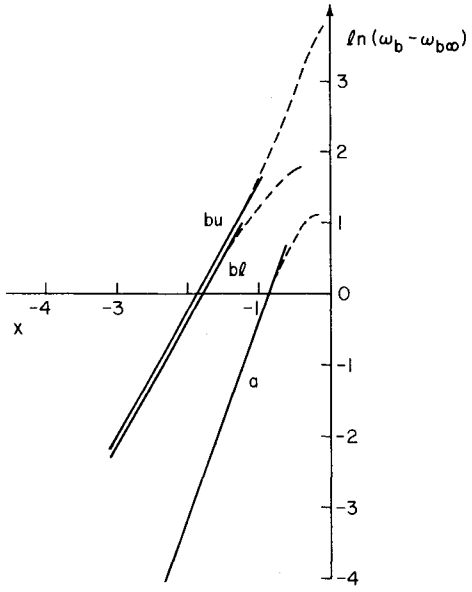

Fig. 6 Exponential decay of vorticity disturbance far upstream ($Re = 400$, $H = 0.5$): *a*, symmetrical constriction, lower wall; *bu*, asymmetrical constriction, upper wall; *bℓ*, asymmetrical constriction, lower wall; *x*, separation point.

Table 1 Comparison of wall vorticity of symmetrical constriction at $Re = 100$, $H = 0.5$, for $NY^a = 21$ and 31

x	y	$NY = 31$	$NY = 21$
−2.306	0.0	−2.9913	−2.9918
−1.447	0.0	−2.8819	−2.8824
−1.051	0.0	−2.6299	−2.6307
−0.763	0.0	−2.1854	−2.1858
−0.549	0.0	−1.5995	−1.5988
−0.392	0.0	−1.0072	−1.0054
−0.197	0.0	−0.1714	−0.1656
−0.151	0.0	−0.0104	−0.0148
−0.086	0.0	0.0667	0.0429
0.0	0.4646	−50.41	−50.27
0.0	0.4932	−131.25	−128.96
0.0	0.4987	−366.45	−364.66
0.0013	0.5	−283.04	−282.43
0.0067	0.5	−53.14	−55.47
0.0143	0.5	−31.245	−31.271
0.0233	0.5	−22.980	−22.846
0.0335	0.5	−18.733	−18.613
0.0444	0.5	−16.271	−16.173
0.0560	0.5	−14.750	−14.669
0.200	0.5	−12.278	−12.283
1.090	0.5	−14.653	−14.674

[a]Number of grid points across channel.

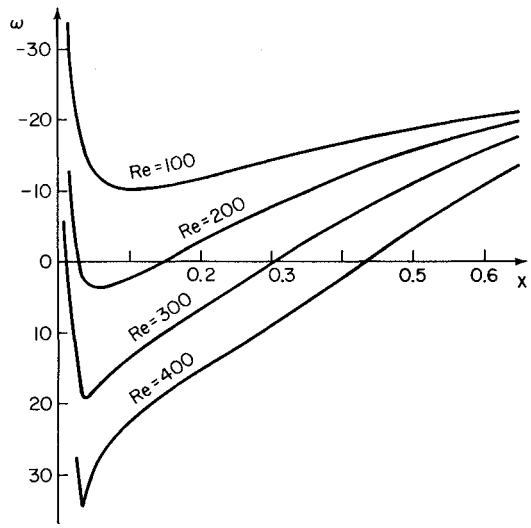

Fig. 7 Vorticity on lower wall after step in asymmetrical constriction ($H=0.5$).

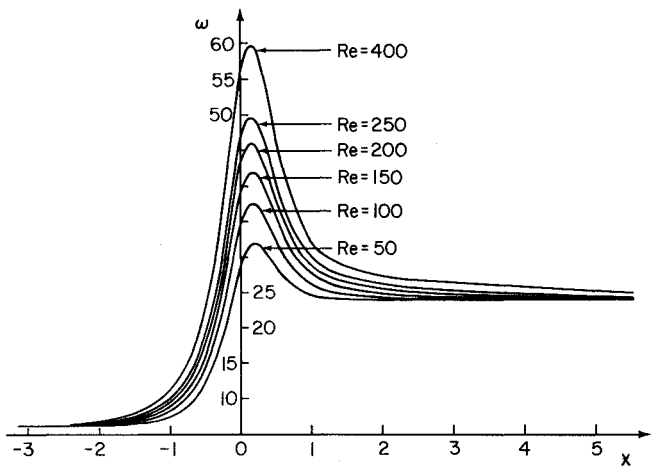

Fig. 8 Vorticity on upper wall for asymmetrical constriction ($H=0.5$).

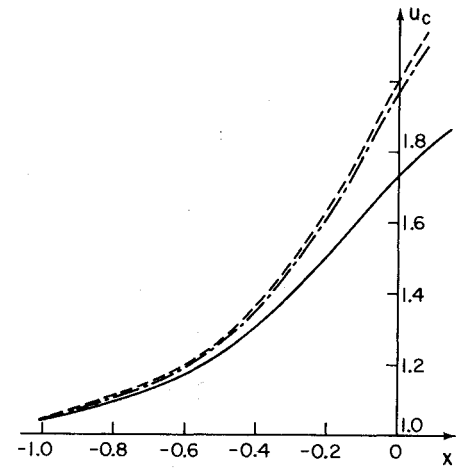

Fig. 9 u-velocity component (at $y=1$) near the step for cascade ($H=0.5$); --- inviscid; —— $Re=100$; —·— $Re=250$.

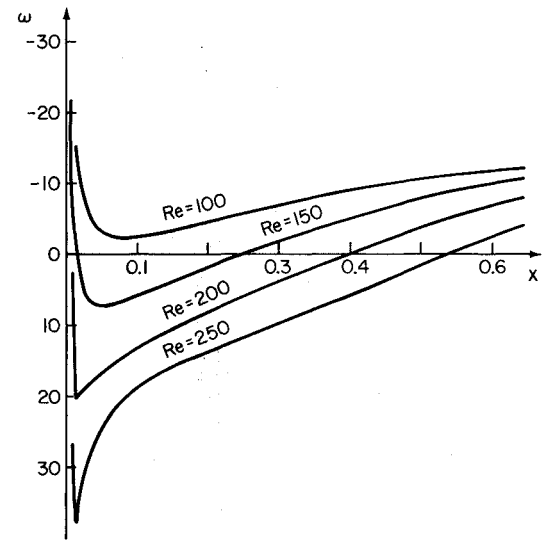

Fig. 10 Wall vorticity after step of cascade ($H=0.5$).

First, the deviation from the initial Poiseuille flow occurs further upstream than in the symmetrical case. For both the symmetrical and asymmetrical cases, the disturbance due to the step decays exponentially far upstream as predicted by asymptotic theory[9] and confirmed by the present computation. That is,

$$(\omega-\omega_\infty)\sim e^{\beta x} \text{ as } x\to-\infty$$

which can be seen in Fig. 6 where $\ln(\omega-\omega_\infty)$ at the wall is plotted vs x for the upper and lower walls of the asymmetrical case and for the lower wall of the symmetrical case for $Re=400$ and $H=0.5$. Along the lower wall, the disturbance due to the asymmetrical constriction decays more slowly than that due to the symmetrical constriction. Also, the upstream separation bubble is larger than in the symmetrical case when Re is slightly greater than 100 for $H=0.5$. Both bubbles increase as Re gets larger but at different speeds, which further indicates the fact that the asymmetric constriction has a stronger upstream interaction.

Second, the flow around the convex corner is more singular than in the symmetrical case, and thus the downstream separation occurs at a smaller value of Re. For both cases, the reattachment point location has a linear dependence on Re as Re gets larger. The wall vorticity after the step is shown in Fig. 7 for $Re=100$-400. As x gets larger, all of these curves asymptotically approach the value of -24. The wall vorticity on the upper wall is shown in Fig. 8. Near $x=0$, the vorticity first decays linearly upstream for small x and then exponentially further upstream, as can be seen in Fig. 6. This agrees with the prediction of Smith[9] for large Re.

Cascade

The flowfield far upstream of the cascade is uniform. As Re gets larger, the upstream interaction becomes much smaller. And indeed, the solution of the Navier-Stokes equations approaches the inviscid solution at some distance upstream of the cascade as Re gets larger as can be expected (see Fig. 9).

The downstream wall vorticity is shown in Fig. 10. The variation of the location of the reattachment points vs Re is shown in Fig. 5. From both of these figures it can be observed that the flow around the convex corner is the most singular of the three flows investigated. The flow separates downstream at Re slightly larger than 110 at $H=0.5$, while $Re\cong 180$ for case II and $Re\cong 230$ for case I. For $Re=300$, the steady solution is no longer obtainable. However, as before, the linearity of x_r vs Re is still clear.

A conventional first-order upwind method is tried for $Re\geq 300$ in order to see the effect of the false diffusion on the flowfield. The flow now becomes steady again but with a much smaller downstream separation bubble, which indicates the decrease in effective Reynolds number. For example, at $Re=500$, the length of the downstream bubble from the

first-order upwind method is about the same as that calculated at $Re=250$ using the present second-order upwind method. The width of the bubble becomes smaller as well.

The central difference method was also used and agreed well with the present analysis for $Re \leq 100$. At $Re=150$ the solution of the vorticity field shows many wiggles for the same mesh, at higher Reynolds numbers no reasonable results could be obtained, and at even higher Reynolds numbers the computation blows up without further decreasing the grid size. This indicates that the central difference method is not suitable for higher Reynolds number flows.

Conclusions

The finite-difference method proposed by Mei and Plotkin[3] is modified by adopting a second-order upwind treatment of the streamwise convection term in the vorticity transport equation. The application of the method to three streamwise convection-dominated flow problems is successful, especially for the solution of the downstream flowfield which is strongly affected by the convex corner. Vortex shedding seems to occur at moderate Reynolds numbers. Numerical schemes with artificial diffusion are not suggested for such flows.

Acknowledgments

The authors wish to thank Professor J. Anderson of the University of Maryland for helpful discussions, and the Computer Science Center of the University of Maryland for supplying computer time.

References

[1]Ghia, K. N., Osswald, G. A., and Ghia, U., "A Direct Method for the Solution of Unsteady Two-Dimensional Incompressible Navier-Stokes Equations," Paper presented at the Symposium on Numerical and Physical Aspects of Aerodynamic Flows, Long Beach, CA, Jan. 1983.

[2]Dennis, S.C.R. and Smith, F. T., "Steady Flow Through a Channel with a Symmetrical Constriction in the Form of a Step," *Proceedings of the Royal Society of London*, Ser. A, Vol. 372, 1980, pp. 393-414.

[3]Mei, R. W. and Plotkin, A., "A Finite-Difference Scheme for the Solution of the Steady Navier-Stokes Equations," to appear in *Computers and Fluids*.

[4]Shyy, W., "A Study of Finite Difference Approximations to Steady State, Convection-Dominated Flow Problems," *Journal of Computational Physics*, Vol. 57, 1985, pp. 415-438.

[5]Briley, W. R., "A Numerical Study of Laminar Separation Bubbles Using the Navier-Stokes Equations," *Journal of Fluid Mechanics*, Vol. 47, Pt. 4, 1971, pp. 713-736.

[6]Dennis, S.C.R. and Hudson, J. D., "A Difference Method for Solving the Navier-Stokes Equations," *Proceedings of the First International Conference on Numerical Methods in Laminar and Turbulent Flow*, Pentech Press, London, July 1978, pp. 69-80.

[7]Smith, F. T., "The Separating Flow Through a Severely Constricted Symmetric Tube," *Journal of Fluid Mechanics*, Vol. 90, Pt. 4, 1979, pp. 725-754.

[8]Castro, I. P., "Numerical Difficulties in the Calculation of Complex Turbulent Flow," *Turbulent Shear Flow I*, edited by F. Durst et al., Springer-Verlag, Berlin, 1979, p. 220.

[9]Smith, F. T., "Upstream Interactions in Channel Flow," *Journal of Fluid Mechanics*, Vol. 79, Pt. 4, 1977, pp. 631-655.